

Extended Coronal Heating and Solar Wind Acceleration Over the Solar Cycle

Steven R. Cranmer, John L. Kohl, Mari Paz Miralles, and Adriaan A.
van Ballegooijen

*Harvard-Smithsonian Center for Astrophysics, 60 Garden Street,
Cambridge, MA 02138, USA*

Abstract. This paper reviews our growing understanding of the physics behind coronal heating (in open-field regions) and the acceleration of the solar wind. Many new insights have come from the last solar cycle's worth of observations and theoretical work. Measurements of the plasma properties in the extended corona, where the primary solar wind acceleration occurs, have been key to discriminating between competing theories. We describe how UVCS/SOHO measurements of coronal holes and streamers over the last 14 years have provided clues about the detailed kinetic processes that energize both fast and slow wind regions. We also present a brief survey of current ideas involving the coronal source regions of fast and slow wind streams, and how these change over the solar cycle. These source regions are discussed in the context of recent theoretical models (based on Alfvén waves and MHD turbulence) that have begun to successfully predict both the heating and acceleration in fast and slow wind regions with essentially no free parameters. Some new results regarding these models—including a quantitative prediction of the lower density and temperature at 1 AU seen during the present solar minimum in comparison to the prior minimum—are also shown.

1 Introduction

After more than a half-century of study, the basic physical processes that are responsible for heating the million-degree corona and accelerating the supersonic solar wind are now beginning to be pinned down. Different mechanisms are probably dominant for different regions (see reviews by Mandrini et al. 2000; Hollweg & Isenberg 2002; Longcope 2004; Aschwanden 2006). For example, it seems increasingly clear that bright EUV and X-ray loops are heated by small-scale, intermittent magnetic reconnection that is driven by the continual stressing of their magnetic footpoints (Klimchuk 2006; Gudiksen 2007).

For the open-field regions that link the corona and the solar wind, there is still disagreement about the relative contributions of different processes (see § 4 below). However, we are rapidly approaching a time when these processes can be included in self-consistent models that can make testable predictions. This paper attempts to summarize some recent work that is helping us to bring observations and theoretical models to the point of straightforward comparison and testing. Because the coronal magnetic field varies so substantially both as a function of position (on the Sun at any one time) and as a function of time (over the solar cycle), there is always a broad range of solar wind source

regions available for comparison with model predictions. In some ways, these variations give us something approaching the turnable “parameter knobs” of a laboratory experiment. This paper emphasizes the example of differences between the previous solar minimum (1996–1997) and the present minimum (2007–2009).

2 Coronal Source Regions

The most definitive link between a particular type of coronal structure (measured via remote sensing) and a specific type of quasi-steady solar wind flow (measured *in situ*) is the connection between large coronal holes and high-speed streams (Wilcox 1968; Krieger et al. 1973). Coronal holes are generally interpreted as bundles of open flux tubes that flare out superradially with increasing distance. Observations from the UVCS instrument on *SOHO* suggest that the range of heights over which the wind’s acceleration occurs in coronal holes can vary greatly, even when the wind at 1 AU is identically fast (Miralles et al. 2001, 2006). The denser slow-speed solar wind appears to come from many different coronal sources. Two regions that are often cited as sources of slow wind are: (1) boundaries between coronal holes and streamers, and (2) narrow plasma “stalks” that extend out from the tops of streamer cusps (e.g., Habbal et al. 1997; Fisk et al. 1998; Wang et al. 2000; Strachan et al. 2002). However, during active phases of the solar cycle there is evidence that slow wind also originates in small coronal holes and active regions (Nolte et al. 1976; Neugebauer et al. 1998; Liewer et al. 2004).

The remainder of this paper will discuss the fast solar wind that emerges from polar coronal holes at solar minimum (Cranmer 2009). However, as the SOHO–23 meeting has demonstrated, not all solar minima are created equal. The morphology of the coronal magnetic field exhibited some interesting differences from the previous minimum to the present minimum. Polar coronal holes on the disk in 2007–2009 are smaller in area (by about 15%) in comparison to those from 1996–1997, and their mean photospheric magnetic fields are lower by about 40% as well (e.g., Kirk et al. 2009; Wang et al. 2009). The magnetic field measured at 1 AU is also lower, but by only about 20% (Smith & Balogh 2008). The streamer belt observed in the extended corona has a broader latitudinal extent than it did in 1996–1997 (Tokumaru et al. 2009). It is likely that this is the result of two contributing factors. (1) The weaker polar field does not exert as much transverse pressure, which acts to confine the streamer belt to low latitudes (see, e.g., Vásquez et al. 2003). (2) There are more small and transient coronal holes at low latitudes during the present minimum; these can also deform the streamer belt. Some likely consequences of the above differences in the coronal magnetic field are discussed below.

3 A Smörgåsbord of Measurements

Low-density coronal holes exhibit a complex array of plasma parameters due to their nearly collisionless nature. As a result, every particle species evolves towards having its own unique temperature, its own type of departure from a Maxwellian velocity distribution, and its own outflow speed. Remote-sensing

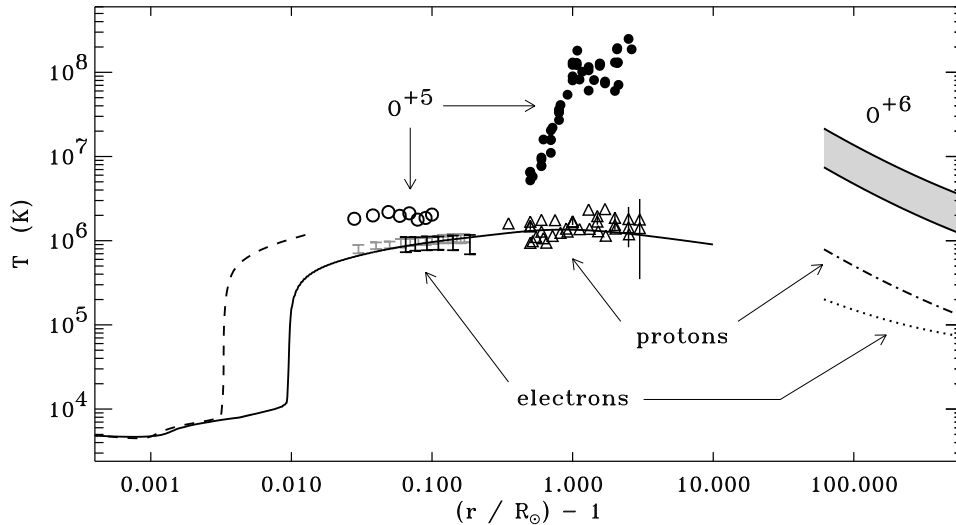


Figure 1. Radial dependence of empirically derived temperatures in polar coronal holes and fast wind streams. See text for details.

measurements of the low corona (i.e., $r \approx 1\text{--}1.3 R_{\odot}$) and the extended corona ($r \approx 1.5$ to $10 R_{\odot}$), as well as *in situ* particle and field detection in the heliosphere ($r > 60 R_{\odot}$), can be combined to follow this evolution. The extended corona is particularly important to study in this regard, since it is not only where most of the wind’s acceleration occurs, but it is also where many plasma species undergo their transition from collisional to collisionless dynamics (see Kohl et al. 2006).

As an example of how different types of measurements can help paint a more complete picture, Figure 1 shows temperature measurements in polar coronal holes from the last solar minimum in 1996–1997. The one-fluid temperatures shown at the lowest heights come from semi-empirical (Avrett & Loeser 2008, dashed curve) and theoretical (Cranmer et al. 2007, solid curve) models of the photosphere, chromosphere, and low corona. Electron temperatures in the low corona were measured by SUMER/*SOHO* and reported by Wilhelm (2006, black bars) and Landi (2008, gray bars). UVCS-derived proton temperatures in the extended corona are also shown (Cranmer 2009, triangles) with an attempt to remove the model-dependent Alfvén wave broadening. Perpendicular temperatures of a representative minor ion (O^{5+}) are shown from SUMER measurements at low heights (Landi & Cranmer 2009, open circles) and UVCS measurements in the extended corona (Cranmer et al. 2008, filled circles). *In situ* electron and proton temperatures in the fast wind (dotted and dot-dashed curves, respectively) are taken from Cranmer et al. (2009). The detailed radial dependences of minor ion temperatures have not yet been precisely measured *in situ*, but the gray region above shows a likely range of values for the abundant O^{6+} ion (see, e.g., Collier et al. 1996).

Coronal holes tend to exhibit preferential ion heating (i.e., $T_{\text{ion}} \gg T_p \gtrsim T_e$) that primarily occurs in the direction perpendicular to the background magnetic field ($T_{\perp} > T_{\parallel}$). Because of these departures from thermal equilibrium, the fast solar wind is an optimal “proving ground” for studies of collisionless kinetic

processes that many believe are the ultimate dissipation mechanisms of coronal heating. It was noticed several decades ago that the damping of ion cyclotron resonant Alfvén waves could naturally give rise to the observed plasma properties (see reviews by Hollweg & Isenberg 2002; Kohl et al. 2006; Cranmer 2009). However, many other dissipation processes have been proposed as well, and they often involve multiple steps of energy conversion between waves, reconnection structures, and other nonlinear plasma features.

4 Coronal Heating and Wind Acceleration

Taking all of the above complexities into account and producing a self-consistent model of coronal heating and solar wind acceleration (for all particle species) has still not been accomplished. However, if an assumption is made to consider only the *total* energy content of the plasma—and not its “partitioning” into protons, electrons, and other ions—then the problem becomes more tractable. At this level of detail, there are two general types of physics-based model that attempt to explain the overall flows of energy:

1. There are *wave/turbulence-driven* (WTD) models in which open magnetic flux tubes rooted to the photosphere are jostled by convection, leading to waves that propagate up into the corona. These waves (usually Alfvén waves) are often proposed to partially reflect back down toward the Sun, develop into strong MHD turbulence, and dissipate over a range of heights. These models also tend to explain the differences between fast and slow solar wind *not* by any major differences in the lower boundary conditions, but instead as an outcome of different rates of lateral flux-tube expansion over several solar radii (Hollweg 1986; Wang & Sheeley 1991; Matthaeus et al. 1999; Ofman 2005; Suzuki & Inutsuka 2006).
2. There are *reconnection/loop-opening* (RLO) models in which the flux tubes feeding the solar wind are influenced by impulsive bursts of mass, momentum, and energy addition. There is often assumed to be strong coupling between closed, loop-like magnetic flux systems (that are in the process of emerging, fragmenting, and diffusing across the surface) and the open flux tubes that connect to the solar wind. These models tend to explain the differences between fast and slow solar wind as a result of qualitatively different rates of flux emergence, reconnection, and coronal heating at the basal footpoints of different regions on the Sun (Axford & McKenzie 1992; Fisk et al. 1999; Fisk 2003; Schwadron & McComas 2003, 2008).

Cranmer et al. (2007) presented a set of WTD models in which the one-fluid equations of mass, momentum, and energy conservation were solved simultaneously with transport equations for Alfvénic and acoustic wave energy. The coronal heating rate was computed self-consistently from a phenomenological description of turbulent dissipation of partially reflected Alfvén waves (see also Matthaeus et al. 1999; Dmitruk et al. 2002; Verdini & Velli 2007). It is important to note that these models were run with lower boundary conditions in the optically thick solar photosphere, and *not* in the transition region (TR) or low corona. Thus, the properties of the chromosphere, the height of the TR, and

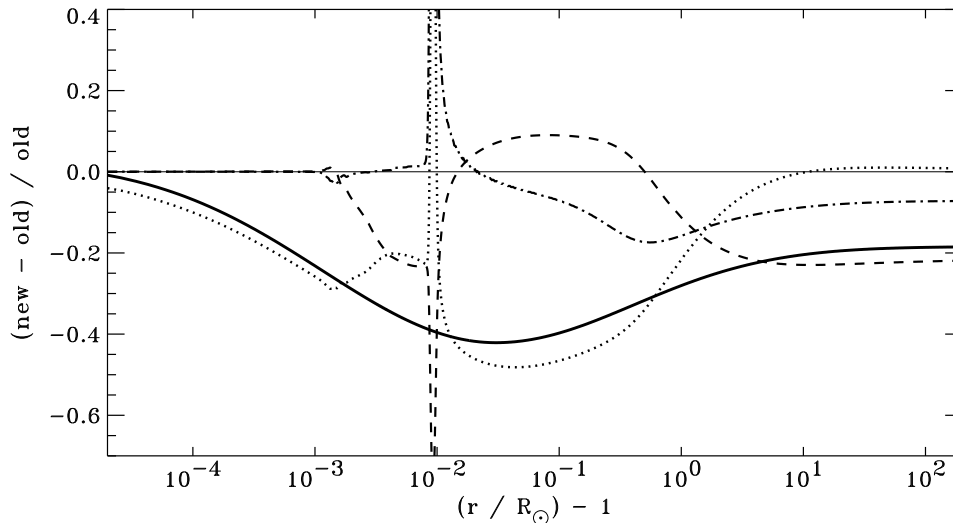


Figure 2. Relative changes in the input magnetic field strength (thick solid curve) and the output solar wind speed (dotted curve), density (dashed curve), and one-fluid temperature (dot-dashed curve), found when comparing the polar coronal model from 1996–1997 (“old”) to that computed for 2007–2009 (“new”). The thin horizontal line denotes the level of zero change. The large variations at $r \approx 1.01 R_{\odot}$ are due to a slight mismatch of the two models in the height of the sharp TR between the chromosphere and the corona.

the mass flux of plasma entering the solar wind were all computed robustly and consistently in these models.

The Cranmer et al. (2007) models of polar coronal holes produced conditions at 1 AU that appeared consistent with fast solar wind measurements at the 1996–1997 solar minimum. More recently, we computed a new set of WTD models that were designed to correspond to the 2007–2009 solar minimum. The *only change* made to the models was in the radial dependence of the imposed magnetic field strength. The Cranmer et al. (2007) magnetic field profile was multiplied by a smooth function constructed to produce the following effects: (1) no change to the ~ 1 kG field strength in the intergranular flux tubes in the photosphere; (2) a 40% reduction in the field strength at the base of the corona ($r \approx 1.03 R_{\odot}$) to account for the lower polar field strengths measured by low-resolution magnetograms; and (3) an 18% reduction in the field strength in interplanetary space from one minimum to the next (see, e.g., Smith & Balogh 2008).

Figure 2 shows the relative changes in the resulting WTD models of polar coronal holes. All quantities are ratios of the form $(X_{\text{new}} - X_{\text{old}})/X_{\text{old}}$, where the subscript “old” refers to the 1996–1997 minimum and “new” refers to the 2007–2009 minimum. The change in the input magnetic field strength, described above, is shown as a solid line. The other quantities are all self-consistent *outputs* of the model. The relative changes at 1 AU can be compared with measured changes in the plasma parameters from McComas et al. (2008) and Ebert et al. (2009). Table 1 shows this comparison and confirms that the modeled solar wind responds in a very similar way to the changing magnetic field as does the actual

solar wind. In both the models and the *Ulysses* polar pass data, the solar wind speed u is relatively unchanged, but the density n and temperature T decrease by factors that hover around 20% and 10%, respectively. The decreases in gas pressure (proportional to nT) and dynamic pressure (proportional to nu^2) are between 20% and 30% for both the observations and models.

Table 1. Relative changes in fast solar wind from 1996–1997 to 2007–2009

	<i>Ulysses</i> polar data	WTD model output
speed	−03%	+01%
density	−17%	−22%
temperature	−14%	−08%
gas pressure	−28%	−21%
dynamic pressure	−22%	−27%

Figure 2 also shows that the models predict the present solar minimum should have a smaller temperature in the low corona and a slightly higher density. Nobeyama measurements of the radio “brightness temperature” (Yashiro et al., this meeting) do indicate a slightly lower temperature in the upper chromosphere during 2007–2009, in comparison to 1996–1997, but there are not yet any firm comparisons from measurements in the low corona. At the heights observable by UVCS, the predicted temperature decline in Figure 2 is about 20% and the predicted density change has shifted from an increase to a slight decrease. (At these heights we expect the proton, electron, and heavy ion temperatures to be behaving differently from one another.) Preliminary reports of minimum-to-minimum variations from UVCS indicate that the H I Ly α intensities are higher in 2007–2009 than in 1996–1997, and the O VI intensities are lower (Gardner et al., this meeting; Miralles et al., this meeting). Both of these changes may be consistent with lower electron temperatures and electron densities, but only detailed empirical modeling of the spectral line properties will reveal whether that is the case.

5 Conclusions

The *SOHO* era has seen significant progress toward identifying and characterizing the physical processes responsible for coronal heating and solar wind acceleration. As remote-sensing measurements have become available in the collisionless extended corona, the traditional gap between solar physics and *in situ* space physics has become narrower. However, there are still many unanswered questions: How and where in the solar atmosphere are the relevant waves and turbulent motions generated? Which kinds of fluctuation modes (i.e., linear or nonlinear; Alfvén, fast, or slow; high k_{\parallel} or high k_{\perp}) are most important? What frequencies dominate the radially evolving power spectrum? What fraction of the interplanetary solar wind comes from filamentary structures such as coronal reconnection events and/or plumes and jets?

Answering the above questions involves moving forward in both the theoretical and observational directions. A key step to making further progress is the

ability to include both the WTD and RLO processes in existing 3D numerical simulations of the Sun-heliosphere system. Some recent progress in producing computationally efficient approximations to the rates of WTD wave reflection has been reported by Chandran & Hollweg (2009) and Cranmer (2010). Studies of the connection between the evolving “magnetic carpet” and the open flux tubes that feed the solar wind are also ongoing.

The plasma parameters of both the major species (protons, electrons, and He^{2+}) and minor ions are not yet known in coronal holes to the accuracy required to determine the relative contributions of the proposed physical processes. As Figure 1 shows, even quantities as basic as the ratio T_p/T_e are not yet known with sufficient accuracy because measurements of the proton and electron temperatures have not yet been made over the same ranges of heights. Minor ion measurements need to be extended to a larger number of ions (i.e., a wider range of ion cyclotron frequencies) so that the ultimate kinetic damping mechanisms of waves and turbulence can be determined (see, e.g., Cranmer 2002). Also, we do not yet have a good enough observational “lower boundary condition” on the energetics of waves and turbulence in the photosphere. Existing measurements of the Sun’s convective granulation with sub-arcsecond spatial resolution need to be matched by sub-second *time resolution*, so that the power spectrum of the motions of small-scale magnetic flux tubes (e.g., G-band bright points) can be extended to higher frequencies.

Acknowledgments. This work was supported by the National Aeronautics and Space Administration (NASA) under grants NNG04GE77G and NNX09-AB27G to the Smithsonian Astrophysical Observatory.

References

- Aschwanden, M. J. 2006, *Physics of the Solar Corona: An Introduction with Problems and Solutions*, 2nd ed. (Berlin: Springer)
- Avrett, E. H., & Loeser, R. 2008, *ApJ Suppl.*, 175, 229
- Axford, W. I., & McKenzie, J. F. 1992, in *Solar Wind Seven*, ed. E. Marsch & R. Schwenn (New York: Pergamon), 1
- Chandran, B. D. G., & Hollweg, J. V. 2009, *ApJ*, 707, 1659
- Collier, M. R., Hamilton, D. C., Gloeckler, G., Bochsler, P., & Sheldon, R. B. 1996, *GRL*, 23, 1191
- Cranmer, S. R. 2002, in *SOHO-11: From Solar Min to Max*, ed. A. Wilson (Noordwijk, The Netherlands: ESA), ESA SP-508, 361
- Cranmer, S. R. 2009, *Living Rev. Solar Phys.*, 6, 3 (arXiv:0909.2847)
- Cranmer, S. R. 2010, *ApJ*, 710, in press
- Cranmer, S. R., Matthaeus, W. H., Breech, B. A., & Kasper, J. C. 2009, *ApJ*, 702, 1604
- Cranmer, S. R., Panasyuk, A. V., & Kohl, J. L. 2008, *ApJ*, 678, 1480
- Cranmer, S. R., van Ballegoijen, A. A., & Edgar, R. J. 2007, *ApJ Suppl.*, 171, 520
- Dmitruk, P., et al. 2002, *ApJ*, 575, 571
- Ebert, R. W., McComas, D. J., Elliott, H. A., Forsyth, R. J., & Gosling, J. T. 2009, *JGR*, 114, A01109
- Fisk, L. A. 2003, *JGR*, 108, 1157
- Fisk, L. A., Schwadron, N. A., & Zurbuchen, T. H. 1998, *Space Sci. Rev.*, 86, 51
- Fisk, L. A., Schwadron, N. A., & Zurbuchen, T. H. 1999, *JGR*, 104, 19765
- Gudiksen, B. V. 2007, in *ASP Conf. Ser. 369, New Solar Physics with Solar-B Mission*, ed. K. Shibata, S. Nagata, & T. Sakurai (San Francisco: ASP), 269

- Habbal, S. R., Woo, R., Fineschi, S., O'Neal, R., Kohl, J., Noci, G., & Korendyke, C. 1997, *ApJ Lett.*, 489, L103
- Hollweg, J. V. 1986, *JGR*, 91, 4111
- Hollweg, J. V., & Isenberg, P. A. 2002, *JGR*, 107 (A7), 1147
- Kirk, M. S., Pesnell, W. D., Young, C. A., & Hess Webber, S. A. 2009, *Solar Phys.*, 257, 99
- Klimchuk, J. A. 2006, *Solar Phys.*, 234, 41
- Kohl, J. L., Noci, G., Cranmer, S. R., & Raymond, J. C. 2006, *A&A Rev.*, 13, 31
- Krieger, A. S., Timothy, A. F., & Roelof, E. C. 1973, *Solar Phys.*, 29, 505
- Landi, E. 2008, *ApJ*, 685, 1270
- Landi, E., & Cranmer, S. R. 2009, *ApJ*, 691, 794
- Liewer, P. C., Neugebauer, M., & Zurbuchen, T. 2004, *Solar Phys.*, 223, 209
- Longcope, D. W. 2004, in *SOHO-15: Coronal Heating*, ed. R. W. Walsh, J. Ireland, D. Danesy, & B. Fleck (Noordwijk, The Netherlands: ESA), ESA SP-575, 198
- Mandrini, C. H., Démoulin, P., & Klimchuk, J. A. 2000, *ApJ*, 530, 999
- Matthaeus, W. H., Zank, G. P., Oughton, S., Mullan, D. J., & Dmitruk, P. 1999, *ApJ Lett.*, 523, L93
- McComas, D. J. et al. 2008, *GRL*, 35, L18103
- Miralles, M. P., Cranmer, S. R., Panasyuk, A. V., Romoli, M., & Kohl, J. L. 2001, *ApJ Lett.*, 549, L257
- Miralles, M. P., Cranmer, S. R., & Kohl, J. L. 2006, in *SOHO-17: 10 Years of SOHO and Beyond*, ed. H. Lacoste, L. Ouwehand (Noordwijk, The Netherlands: ESA), ESA SP-617, 15.1
- Neugebauer, M., et al. 1998, *JGR*, 103, 14587
- Nolte, J. T., et al. 1976, *Solar Phys.*, 46, 303
- Ofman, L. 2005, *Space Sci. Rev.*, 120, 67
- Schwadron, N. A., & McComas, D. J. 2003, *ApJ*, 599, 1395
- Schwadron, N. A., & McComas, D. J. 2008, *ApJ Lett.*, 686, L33
- Smith, E. J., & Balogh, A. 2008, *GRL*, 35, L22103
- Strachan, L., Suleiman, R., Panasyuk, A. V., Biesecker, D. A., & Kohl, J. L. 2002, *ApJ*, 571, 1008
- Suzuki, T. K., & Inutsuka, S.-I. 2006, *JGR*, 111, A06101
- Tokumar, M., Kojima, M., Fujiki, K., & Hayashi, K. 2009, *GRL*, 36, L09101
- Vásquez, A. M., van Ballegooijen, A. A., & Raymond, J. C. 2003, *ApJ*, 598, 1361
- Verdini, A., & Velli, M. 2007, *ApJ*, 662, 669
- Wang, Y.-M., Robbrecht, E., & Sheeley, N. R., Jr. 2009, *ApJ*, 707, 1372
- Wang, Y.-M., & Sheeley, N. R., Jr. 1991, *ApJ Lett.*, 372, L45
- Wang, Y.-M., Sheeley, N. R., Socker, D. G., Howard, R. A., & Rich, N. B. 2000, *JGR*, 105, 25133
- Wilcox, J. M. 1968, *Space Sci. Rev.*, 8, 258
- Wilhelm, K. 2006, *A&A*, 455, 697